

# Linear Load Transfer Based Horizontal Motion Control of a ROV

Kerim Deniz Kaya  
Department of Marine Engineering  
Dokuz Eylul University  
İzmir, Turkey

Aytaç Gören  
Department of Mechanical Engineering  
Dokuz Eylul University  
İzmir, Turkey

**Abstract**— In this study, an electromechanical design and a proper control architecture has been proposed for horizontal motion control of a remote operated underwater vehicle. Horizontal motion is performed with the combination of roll and yaw rotations. With the use of mathematical model and dynamic equations of the remote operated vehicle, control architecture has been developed for auto-tuning the position of a linear brushless direct current motor and angular velocities of horizontal thrusters. In particular, the part of control architecture related with roll rotation tuning through the linear motion of a mass along pitch axis has been accentuated in this paper. Control system has been realized as a MATLAB/Simulink simulation model thus the responses have been monitorized. Finally, series of performance analysis over tracking capabilities have been carried out.

**Keywords**—underwater vehicle; motion control; linear actuation

## I. INTRODUCTION

At the present time, control and design of underwater robots has become a significant scientific field of study arising from intense effort in underwater applications such as ship maintenance, port operations, hydroelectric energy systems, underwater pipelines, salvage services and underwater exploration. All of these working fields have some requirement of unmanned underwater operations for industrial, military or scientific purpose. Like other land, aerial or marine type of unmanned vehicles, underwater vehicles have a series of mission specification and working environment. Possible working fields of underwater robots given as follows [1].

TABLE I. APPLICATIONS OF UNDERWATER ROBOTS

Field	Application
Science	<ul style="list-style-type: none"> <li>Seafloor Mapping</li> <li>Rapid response to oceanographic and geothermal events</li> <li>Geological sampling</li> </ul>
Environment	<ul style="list-style-type: none"> <li>Long term monitoring (e.g., hydrocarbon spills, radiation leakage, pollution)</li> <li>Environmental remediation</li> <li>Inspection of underwater structures including pipelines, dams, etc.</li> </ul>
Military	<ul style="list-style-type: none"> <li>Shallow water mine search and disposal</li> </ul>

Field	Application
	<ul style="list-style-type: none"> <li>Submarine off-board sensors</li> </ul>
Ocean Mining and Oil Industry	<ul style="list-style-type: none"> <li>Ocean survey and resource assessment</li> <li>Construction and maintenance of undersea structures</li> </ul>
Other applications	<ul style="list-style-type: none"> <li>Ship hull inspection and ship tank internal inspection</li> <li>Nuclear power plant inspection</li> <li>Underwater communication &amp; power</li> <li>cables installation and inspection</li> <li>Entertainment-underwater tours</li> <li>Fisheries-underwater ranger</li> </ul>

## II. PROBLEM AND SYSTEM DESCRIPTION

As it is seen in Figure 1, robots and vehicles which navigate in underwater environment have six degree of freedoms [2]. In order to follow the predetermined pathways and respond to the real time motion commands there should be some control over these degree of freedoms. The objective of the control architecture in this study is to create a maneuvering capability along horizontal plane due to tuning of the roll rotation.

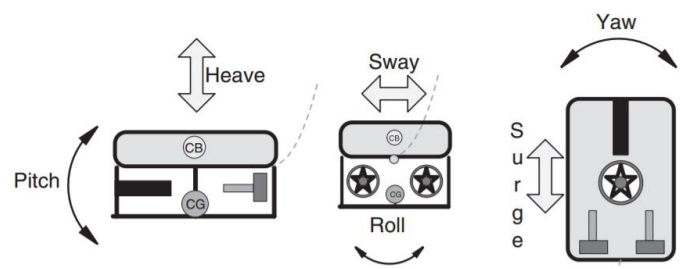


Fig. 1 Underwater Vehicle Degree of Freedoms

Roll rotation is planned to be performed through a moving mass which is actuated by a linear brushless direct current motor. LBDCM is located inside the ROV. Rotor and stator axes are located coincident with pitch axis. The settlement of LBDCM inside the ROV can be seen in Figure 2.

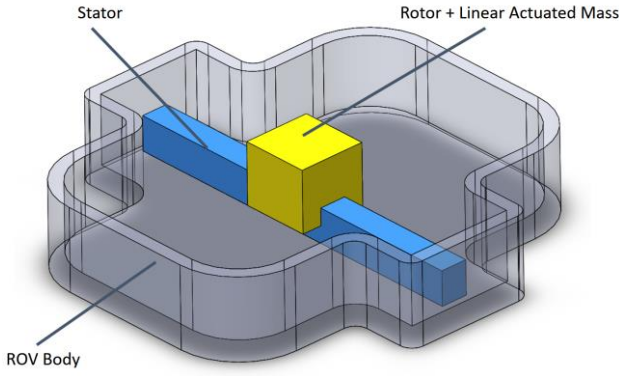


Fig.2 Settlement of Linear Actuation

### III. ROV MODELLING

#### A. Kinematic Model of Underwater Robot

In order to determine the control parameters of ROV, the kinematic model of the system should be created. The motion is defined according to earth fixed frame and body fixed frame as seen in Figure 3.

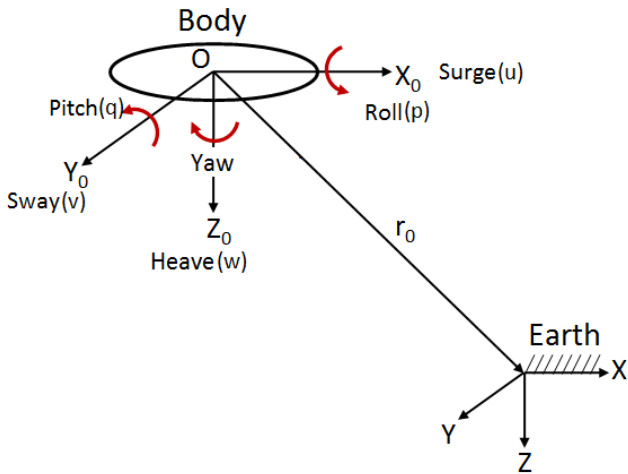


Fig. 3 Earth and Body Fixed Frames

Body fixed frame is located at the center of gravity thus linear and angular velocity data are described according to body fixed frame. On the other side position and orientation data are described according to the earth fixed frame [3][4].

In the light of this information, the vectors that express the motion through six axes are indicated below [5].

$$\begin{aligned} \eta &= [\eta_1^T, \eta_2^T]^T; \eta_1 = [x, y, z]^T; \eta_2 = [\phi, \theta, \varphi]^T \\ v &= [v_1^T, v_2^T]^T; v_1 = [u, v, w]^T; v_2 = [p, q, r]^T \\ \tau &= [\tau_1^T, \tau_2^T]^T; \tau_1 = [X, Y, Z]^T; \tau_2 = [K, M, N]^T \end{aligned} \quad (1)$$

Here,  $\eta$  is the combination of position and orientation vectors described according to earth-fixed frame,  $v$  is the combination of linear and angular velocity vectors described according to body-fixed frame and  $\tau$  is the combination of moment and force vectors acting on ROV. In particular, Euler angles( $\phi, \theta, \varphi$ ) are significant due to their function of describing the orientation and defining the control parameters.

Linear velocity transformation with respect to earth-fixed frame is given as follows [6]:

$$\dot{\eta}_1 = J_1(\eta_2)v_1 \quad (2)$$

Here  $J_1(\eta_2)$ , is the transformation matrix that is related with Euler angles.

$$J_1(\eta_2) = \begin{bmatrix} c\varphi c\theta & -s\varphi c\theta + c\varphi s\theta s\phi & s\varphi s\theta + c\varphi c\theta s\phi \\ s\varphi c\theta & c\varphi c\phi + s\varphi s\theta s\phi & -c\varphi s\phi + s\theta s\varphi c\phi \\ -s\theta & c\theta s\phi & c\theta c\phi \end{bmatrix} \quad (3)$$

Angular velocity vector with respect to the body-fixed frame is associated with Euler vector through  $J_2(\eta_2)$  transformation matrix.

$$\dot{\eta}_2 = J_2(\eta_2)v_2 \quad (4)$$

$J_2(\eta_2)$  transformation matrix can be written in terms of Euler angles as follows:

$$J_2(\eta_2) = \begin{bmatrix} 1 & s\phi\theta & c\phi\theta \\ 0 & c\phi & -s\phi \\ 0 & s\phi/c\theta & c\phi/c\theta \end{bmatrix} \quad (5)$$

#### B. Dynamic Model of Underwater Robot

$$\begin{aligned} M\dot{v} + C(v)v + D(v)v + g(\eta) &= \tau \\ \dot{\eta} &= J(\eta)v \end{aligned} \quad (6)$$

Here,  $M$  is the sum of  $M_{RB}$  rigid body mass matrix and  $M_A$  added mass matrix.  $C(v)$  is the sum of  $C_{RB}(v)$  rigid body Coriolis matrix and  $C_A(v)$  added mass Coriolis matrix.

$$\begin{aligned} M &= M_{RB} + M_A \\ C(v) &= C_{RB}(v) + C_A(v) \end{aligned} \quad (7)$$

$D(v)$ ,  $g(\eta)$  and  $\tau$  are damping matrix, gravity and lifting force vector and input vector respectively.

#### IV. LINEAR MOTION BASICS

##### A. Linear Brushless Direct Current Motor Model

Lorentz force parameter in electric motors is the basis of LBDCM mathematical model. Instead of nominal torque, there is nominal force:

$$\vec{F} = q \cdot \vec{v} \times \vec{B} \quad (8)$$

If the variations of the stator self-inductance with rotor position and the mutual inductance between stator windings considered as negligible; electrical dynamics of LBDCM may be modeled as an electrically balanced system [7].

$$u_{si} - V_0 = L_s \frac{di_{si}}{dt} + R_s i_{si} + e_i; \quad i=1,2,3 \quad (9)$$

$$\sum i_{si} = 0 \quad (10)$$

In (9),  $R_s$  and  $L_s$  are the stator resistance and inductance,  $u_{si}$  is the motor terminal voltage,  $i_{si}$  is the phase current and  $e_i$  is the back-EMF associated with the  $i$ th phase. The potential of the motor neutral terminal in wye-connected windings is denoted as  $V_0$ . The back-EMF induced in each phase;

$$e_i = \frac{d\psi_{ir}}{dt} = \frac{\partial \psi_{ir}}{\partial \theta} \frac{d\theta}{dt} = \omega \frac{\partial \psi_{ir}}{\partial \theta} \quad (11)$$

If  $\psi_{ir}$  is the mutual magnetic flux between the permanent magnet and the stator windings in the  $i$ th phase,  $\theta$  is the rotor position, and  $\omega$  is the rotor speed. If the model is assumed as linear;

$$d\psi_{ir} = L_{ir} i_r \quad (12)$$

The mutual inductance  $L_{ir}$  is expressed, using the terms of the trigonometric Fourier series, as:

$$L_{ir} = \sum_{k=1}^K [L_{irak} \cos k(p\theta - \frac{2\pi}{3}(i-1)) + L_{irbk} \sin(p\theta - \frac{2\pi}{3}(i-1))] \quad (13)$$

The back EMF can be derived from (11) and (12) as;

$$e_i = i_r \omega \frac{\partial L_{ir}}{\partial \theta} \quad (14)$$

The electromagnetic motor torque can be derived as;

$$T = \sum_{i=1}^3 T_i + T_{icogg} = i_r (\sum_{i=1}^3 i_{si} \frac{\partial L_{ir}}{\partial \theta}) + \frac{1}{2} i_r^2 \frac{\partial L_{rr}}{\partial \theta} \quad (15)$$

The first three terms in (15) are mutual torques caused by interaction between the permanent magnet field and the phase currents.  $T_{icogg}$  is the cogging-torque, due to the attraction of the permanent to the salient portions of the stator iron. So, even in the absence of the phase currents, the cogging-torque is present.

If  $T_l$  is the load torque,  $J$  is the rotor inertia,  $B$  is the viscous friction coefficient  $C$  is the Coloumb friction coefficient, mechanical dynamics model of the motor is defined as;

$$\dot{\theta} = \omega; \quad \dot{\omega} = \frac{1}{J} (T - T_l - B\omega - C \text{sign}(\omega)) \quad (16)$$

##### B. Structure of Linear Brushless Direct Current Servo Motor

The LBDCSM (linear brushless direct current servo motor) is designed as a brushless motor which has a wye connected windings in stator. The motor has three wires those are connected to three phases from driver which follow each other with  $120^\circ$ . The motor driver gets the feedback signal from three Hall - Effect sensors those are located on the stator unit (Fig. 4 and Fig. 5).

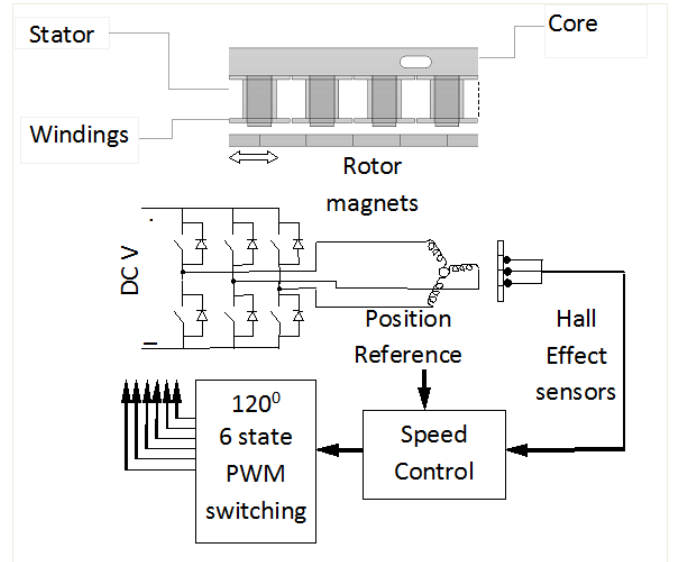


Fig 4. Structure of the LBDCSM and its driver.

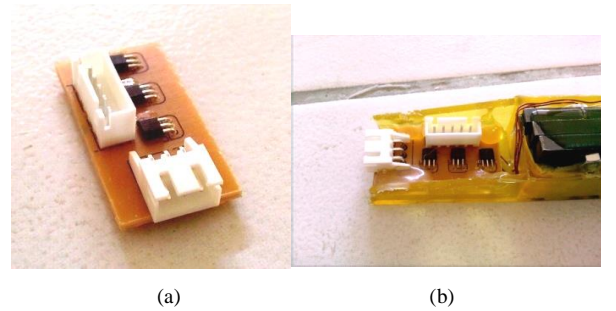


Fig. 5. (a) Hall-effect sensor card, (b) the sensor card placed on the stator unit

The signals from Hall-Effect sensors (HES) are processed to have position data. The structure is not so different from a rotating brushless motor, but in fact the rotor and stator are just became lines parallel to each other.

## V. POSITION CONTROL ALGORITHM

### A. Design of LBDCSM Driver

The designed driver of the system is a six state switching motor driver. According to the data taken from sensors, the driver generates PWM signals and drives the appropriate phase or phases due to the rotor position.

The sensor data taken from the Hall – Effect sensors are evaluated in two stages in motor drive algorithm. First, the position data is generated. Second is the information which one of the six states needed to be applied to stator phases of the motor (see Table 2)

TABLE 2. THE CONTROL LOGIC OF PHASES DUE TO THE POSITION OF ROTOR MAGNETS

Sensor Output			Rotor Position			Motor Forward			Motor Backward		
A	B	C	A	B	C	A	B	C	A	B	C
0	1	0	0	1	1	0	1	0	0	0	1
0	1	1	0	0	1	0	1	1	1	0	1
0	0	1	1	0	1	0	0	1	1	0	0
1	0	1	1	0	0	1	0	1	1	1	0
1	0	0	1	1	0	1	0	0	0	1	0
1	1	0	0	1	0	1	1	0	0	1	1

### B. Positioning Algorithm

Position data and reference position data are processed in control algorithm to get the appropriate PWM signal for the motor. Subsequently, PWM parameters and switching sequence data are processed in motor driver algorithm and sent to the stator of the motor. The change in position affects the sensors, so a closed loop control is formed as seen in Fig.6.

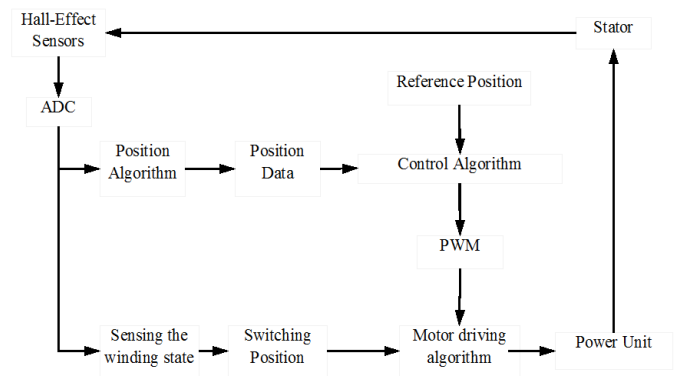


Fig.6 Structure of the control algorithm.

## VI. SIMULATION RESULTS AND CONCLUSIONS

Closed loop control cycle which comprises the proposed control method and the model blocks of LBDCSM, hall effect sensor pack, PWM driver will be built in Matlab/Simulink environment. Simulation results will be obtained as system responses and tracking capabilities. LBDCSM parameters will be observed in terms of rotor speed, electrical power, mechanical power, supply current and efficiency.

### REFERENCES

- [1] J. Yuh, "Design and Control of Autonomous Underwater Robots: A Survey" *Autonomous Robots*, Cilt: 8, No: 1, s:7-24, 2000
- [2] Robert D. Christ and Robert L. Wernli Sr, *The ROV Manual A User Guide for Observation-Class Remotely Operated Vehicles*, Elsevier, 2007, pp.11-45.
- [3] M. Caccia, "Vision-Based ROV Horizontal Motion Control: Near-Sea-floor Experimental Results" *Control Engineering Practice*, s:703-714, 2007
- [4] T. I. Fossen, *Guidance and Control of Ocean Vehicles*, John Wiley&Sons, 1994.
- [5] S.K. Kartal, M.K. Leblebicioğlu, "Bir insansız sualtı aracının yer tespiti ve güdümü" *Otomatik Kontrol Ulusal Toplantısı(TOK 2014)*, Kocaeli, Türkiye,s:713-720,2014
- [6] R. Ramesh, N. Ramadas, D. Sathianarayanan, N. Vedachalam, G.A. Ramadas, "Heading Control of ROV ROSUB6000 Using Non-Linear Model-Aided PD Approach", *International Journal of Emerging Technology and Advanced Engineering*, Cilt: 3, No:4, s:382-393, 2013
- [7] A. Kapun, M. Curkovic, A. Hace, K. Jezernik, "Identifying dynamic model parameters of a BLDC motor", *Simulation Modeling Practice and Theory*, Vol. 16, pp. 1254–1265, 2008.